# Degradation of palmitic (hexadecanoic) acid deposited on $TiO_2$-coated self-cleaning glass: kinetics of disappearance, intermediate products and degradation pathways

**Virginie Roméas,[a] Pierre Pichat,*[a] Chantal Guillard,[a] Thierry Chopin[b] and Corinne Lehaut[b]**

[a] *URA au CNRS "Photocatalyse, Catalyse et Environnement" Ecole Centrale de Lyon, BP 163, 69131 Ecully CEDEX, France. E-mail: Pierre.Pichat@ec-lyon.fr*
[b] *Rhône-Poulenc, Centre de Recherches, 93308 Aubervilliers CEDEX, France*

***Received (in Montpellier, France) 13th July 1998, Revised manuscript received 17th February 1999, Accepted 18th February 1999***

Self-cleaning glass was prepared by depositing anatase nanoparticles as a transparent film onto glass previously coated by a barrier layer. A photoreactor was built to evaluate the efficiency. Palmitic acid, chosen as a compound representing stains from various sources and sprayed over these plates to form an uniform layer of *ca.* 580 nm thickness, was shown to disappear at a rate of *ca.* 60 nm $h^{-1}$ under UV irradiation corresponding to the average solar radiant power at midlatitude. That clearly demonstrated that this glass is efficient enough, at least with this type of grease stain, to implement its use. Our main efforts explored the identification of palmitic acid degradation products under these conditions by use of chromatographic methods, various solvents for recovering products on the glass, and various adsorbents (cartridges or SPME) for gas-phase analysis. The 39 products identified revealed the gradual splitting of the palmitic acid chain yielding the whole series of linear aldehydes and carboxylic acids, some alkanes and two alcohols. In the closed photoreactor, complete mineralization was achieved. When the photoreactor atmosphere was renewed every hour, formaldehyde, acetaldehyde and acetone reached the highest concentrations in the gas phase. Mechanisms involving the initial attack of palmitic acid either by photogenerated holes or by hydroxyl radicals with subsequent formation of alkylperoxy radicals, hydroperoxides and tetroxides are discussed to account for the products.

## 1 Introduction

UV-irradiated $TiO_2$ is able to destroy organic molecules present on its surface, which represents a further potential application of heterogeneous photocatalysis.[1] Therefore deposition of $TiO_2$ as a film on glass or ceramics panes has been proposed for obtaining self-cleaning surfaces. For that purpose, methods to deposit a transparent, abrasion resistant and photocatalytically efficient $TiO_2$ thin film onto glass surfaces have been recently reported.[2–4] Some processes have been patented.[5,6] The Japanese firm Toto has developed both anti-bacterial ceramic tiles and glass plates coated with $TiO_2$.[7] In Fujishima's group[8] and Heller's group[9] glass plates have been prepared and shown to clean themselves from grease and tobacco stains or from coffee stains, respectively.

The objectives of our research were (i) to further assess the efficiency of transparent glass plates, coated by a thin $TiO_2$-containing film, in making a $C_{15}H_{31}CO_2H$ sprayed layer disappear under UV-A irradiation; and (ii) to identify and, if possible, quantify the intermediate products formed during the destruction of the palmitic acid layer in order both to complete the data concerning the self-cleaning properties of the glass plates and to give an insight into the photocatalytic degradation pathways.

Palmitic acid was selected for several reasons. First, this compound is the most abundant fatty acid in human sebum[10] and is thus present in finger marks. A further clue of the presence of palmitic acid on articles handled manually was found in a study of chromatographic 'ghost peaks'[11] which indicated that they are due to finger fatty acids, especially palmitic acid, deposited on the syringe needle by the experimenter. Second, palmitic acid is emitted during the cooking of some foodstuffs, particularly meat;[12] it can therefore be regarded as a good representative of grease stains that can be found on the inner side of window panes. Third, it is also found in tobacco smoke particulate phase (10–155 μg per cigarette).[13] Fourth, analyses of tropospheric solid particles in the Los Angeles area[14] showed that palmitic acid is the most abundant compound (100–250 ng $m^{-3}$) among the identified organics (*ca.* 1000 ng $m^{-3}$). Sources include the combustion of fossil fuels, wood and organic detritus; particles containing *n*-alkanoic acids, among which palmitic acid, also result from leaf surface waxes which are blown up by winds. Therefore, dry or wet deposition of these atmospheric particles onto the outer side of window panes can contribute to the presence of palmitic acid in the solid layers that blur the sight through the glass.

Finally, as it contains only a saturated hydrocarbon linear chain and a $CO_2H$ group that are both quite stable, palmitic acid is a good candidate to test the capabilities of the self-cleaning glass plates.

The photocatalytic degradation of octadecanoic (stearic) acid on $TiO_2$ thin films attached on glass has been studied by Sitkiewitz and Heller.[15] The formation of $CO_2$ was monitored but no degradation intermediate products were searched for. These $TiO_2$ films were found to be effective in the complete removal of 200 nm-thick layers of stearic acid.

In this study, we have shown the efficiency of glass plates whose photocatalytic coating was prepared from nanoparticles synthesized by Rhône-Poulenc. We have identified numerous products of the degradation of palmitic acid and also evaluated to what extent some of these products can be rel-

eased in the atmosphere. To our knowledge, these essential aspects regarding the fate of an organic layer deposited on a $TiO_2$ coating submitted to solar light are explored for the first time. Photocatalytic degradation pathways are tentatively proposed and discussed.

## 2 Experimental

### 2.1 Materials

Palmitic acid (99%) was purchased from Sigma and its degradation intermediate products from Aldrich, Fluka or Merck. All these products were used as received.

The glass coating was prepared from $TiO_2$ nanoparticles ($>250$ $m^2$ $g^{-1}$) synthesized by Rhône-Poulenc and a photostable binder. The solution was deposited *via* the dip-coating method. The coated plates were then annealed at a temperature higher than 623 K. The mass ratio $TiO_2$/photostable binder was 80/20. The layer was roughly 45 nm thick, had an anatase crystalline structure, and was hydrophilic. SEM photographs of the $TiO_2$ thin layers are shown in Fig. 1.

### 2.2 Palmitic acid deposition

Palmitic acid was deposited (Fig. 2) by spraying (system: Jet Pack Spray Gun, Bioblock) a 8 g $L^{-1}$ chloroformic solution of this compound. Approximately 1.5 mg of palmitic acid was sprayed on each plate, *i.e. ca.* 0.2 μmol $cm^{-2}$ or 50 μg $cm^{-2}$ which corresponded to a layer of *ca.* 580 nm thick as calculated from the density of palmitic acid at 335 K. Reproducibility in the deposited amount was evaluated to be $\pm 15\%$ under somewhat optimized conditions (nature of the solvent; palmitic acid concentration; distance between the gas container and the glass plate; angle α, Fig. 2). These deposits exhibited a regular and uniform visual aspect; no attempt was made to determine the uniformity of the layer thickness along the glass plate. The palmitic acid disappearance rates given in the results section correspond to a calculated mean value of the deposit thickness.

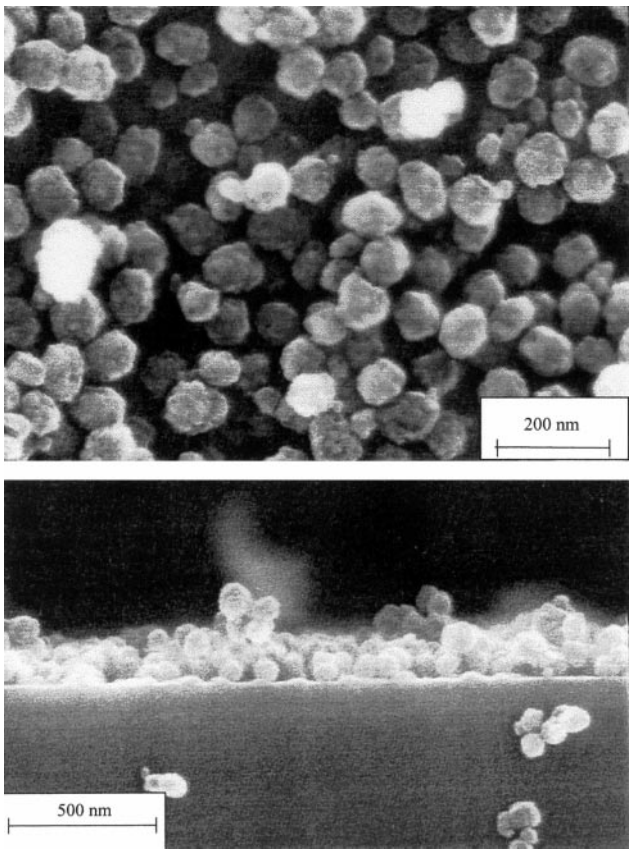


**Fig. 1** SEM photographs of $TiO_2$ nanoparticles deposited on glass, (a) top view, (b) side view.

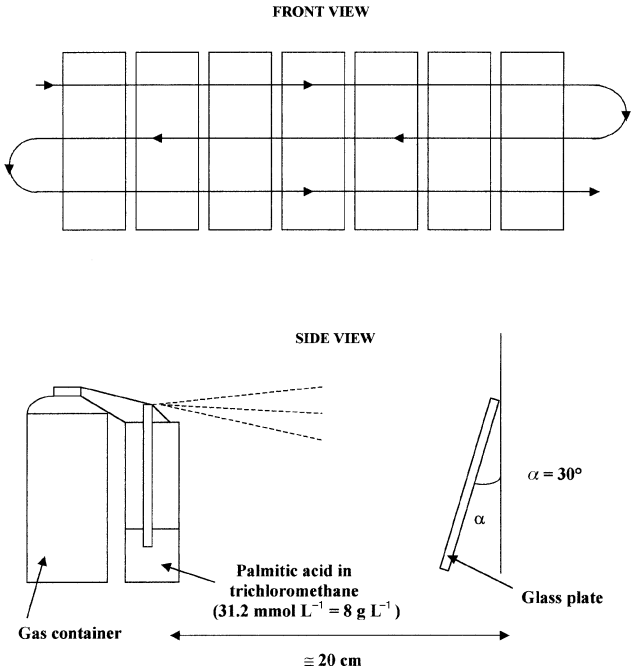


**Fig. 2** Illustrations showing the method by which palmitic acid is deposited on glass plates.

### 2.3 Photoreactor and light sources

A photoreactor of *ca.* 2.2 L (Fig. 3) was designed and constructed to study the photodegradation of the thin palmitic acid layers covering the $TiO_2$-coated glass substrates. Five glass plates (10 cm long, 3 cm wide and 4 mm thick) were vertically disposed at equal distance (*ca.* 35 mm) from the axis

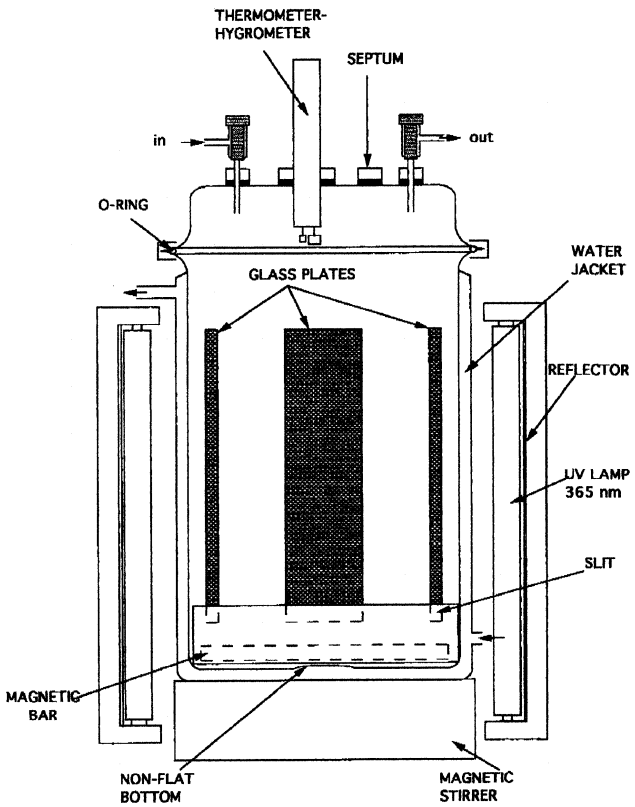


**Fig. 3** Photoreactor used in this work.

of the cylindrical reactor. They were fixed in slits drilled in a Teflon disk, which was magnetically rotated (*ca.* 20 rpm) to ensure a regular mean irradiation of the glass plates. In some cases, the reactor was filled with dioxygen (purity >99.998%, HP 48 Carboxyque, France) and closed before starting UV irradiation; in other cases, a 50 mL $min^{-1}$ dioxygen flow was circulated through the reactor during the photocatalytic degradation. The relative humidity of the inner atmosphere was kept between 50 and 80% by adding a few drops of pure water in a hole drilled in the Teflon disk. Six Philips TL 29D/16 09N UV tubular lamps (Fig. 4) were vertically and regularly placed in a circle outside the reactor at about 2 mm from the external wall. They emitted in the 315–400 nm range with a maximum at 365 nm. A circulating water jacket kept the temperature between 291 and 295 K inside the reactor. The average radiant flux reaching the glass plates, measured by use of a UDT 21 A powermeter, was found to be between 7 and 10 W $m^{-2}$, *i.e.* of the same order of magnitude as the average solar radiant power on a horizontal plane at mid-latitudes for wavelengths $\leqslant$380 nm.[16,17]

## 2.4 Analyses

**2.4.1 Measurements of the palmitic acid amounts.** To measure the amount of palmitic acid deposited on the glass plates, these plates were washed with 5 mL of chloroform containing 200 mg $L^{-1}$ of dodecanoic acid (used as internal standard). The resulting solution was analyzed with a Varian 3400 gas chromatograph equipped with a flame ionization detector and a CP Sil 5 CB column (25 m long, 0.32 mm i.d., 1.2 μm film thickness).

**2.4.2 Detection of the organic intermediate products on the glass plates.** In a first series of experiments, the $TiO_2$-coated glass plates, initially covered with *ca.* 1.5 mg palmitic acid and UV irradiated for 3 h in the photoreactor under an $O_2$ flow, were immersed in 200 mL of a 2 g $L^{-1}$ NaOH aqueous solution. After 15 min sonication (40 Hz), the solution was concentrated in a rotary evaporator down to 5 mL and then acidified (pH = 2) with phosphoric acid before being analyzed by HPLC. The HPLC apparatus comprised a LDC Constametric 3000 isocratic pump, a Waters 486 UV Detector set at 210 nm and a 20 μL injection loop. A Spherisorb ODS 2 column (25 cm long, 4.6 mm i.d., 5 μm particles diameter) was used. The mobile phase (flow rate: 1 mL $min^{-1}$) was deionized, doubly-distilled water (Milli-Q system) containing 10 mmol $L^{-1}$ phosphoric acid.

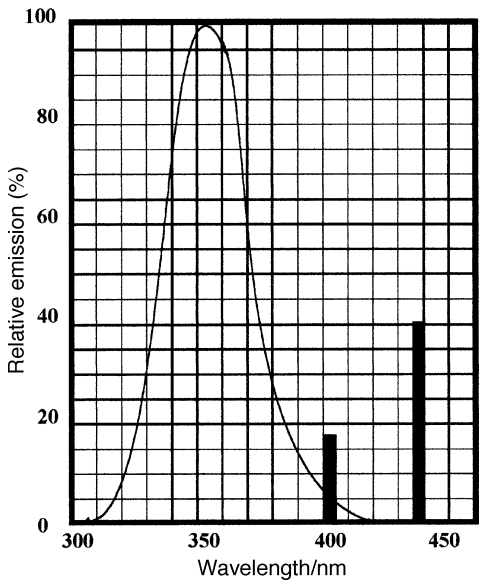


**Fig. 4** Spectral emission of the Philips TL 29 D 16/09 N lamp (according to the manufacturer).

In another series of experiments, the $TiO_2$-coated glass plates, also initially covered with *ca.* 1.5 mg palmitic acid, were irradiated for durations comprised between 30 min and 3 h in the closed photoreactor. After each irradiation duration, the $TiO_2$-coated side of each of the five plates was washed with 5 mL $CH_2Cl_2$ (Pestinorm grade) which was not enough to collect all the organic matter remaining on the glass but enabled the subsequent GC-MS analysis to be carried out without further concentration. This solution was analyzed with a HP 5890 series II gas chromatograph equipped with a CP Sil 5 CB column (25 m long, 0.25 mm i.d., 1.2 μm film thickness); the temperature was programmed from 348 to 513 K at 15 K $min^{-1}$, hold time: 13 min. Detection and identification were performed with a HP 5971A MS detector using the electron ionization mode. The major organic compounds in the sample were initially identified by computer matches to standard reference mass fragmentograms in the NBS 49K library and the identifications were checked later by compariscon with standards.

In both cases, control analyses were performed in which the same procedures were used but without irradiating the glass plates.

**2.4.3 Detection of the organic intermediate products in the gas phase.** *Case of the photoreactor through which a 50 mL $min^{-1}$ $O_2$ flow was circulated.* An ORBO 32 (Supelco) activated charcoal cartridge was placed in the gaseous output of the photoreactor during the irradiation. At the end of the irradiation period, the activated charcoal was transferred into a vial containing 1 mL Pestinorm grade dichloromethane and manually shook during 1 min. No filtration was carried out in order to avoid the loss of analytes. This solution was analyzed with the GC-MS apparatus equipped with the same CP Sil 5 CB column; the column temperature was programmed from 311 to 403 K at 3 K $min^{-1}$ and from 403 to 493 K at 20 K $min^{-1}$.

To detect carbonyl compounds, two Supelco Lp DNPH10 cartridges were connected in series in the gaseous output of the photoreactor during the irradiation. These cartridges contained silica coated with 2,4-dinitrophenylhydrazine (2,4-DNPH) which converts carbonyl compounds into their 2,4-dinitrophenylhydrazone derivatives.

Only one glass plate coated with a low amount of palmitic acid was irradiated in this case in order to avoid sample breakthrough. At the end of the irradiation, the cartridges were each eluted with 4 mL HPLC grade acetonitrile. The resulting solution was then analyzed by reversed phase HPLC under the following conditions: solvent delivery system: Varian 9010; column: Spherisorb ODS2 (25 cm × 4.6 mm i.d., 5 μm particles); mobile phase: A: acetonitrile (30%)–tetrahydrofuran (10%)–water (60%), B: acetonitrile (60%)–water (40%), 100% A for 1 min, linear gradient to 100% B over 10 min, hold time 30 min; flow rate: 1.5 mL $min^{-1}$; injected volume: 20 μL; detector: UV Varian 9065 Polychrom set at $\lambda$ = 360 nm. A standard mixture of derivatized carbonyl compounds (Supelco TO11/IP6A Carbonyl DNPH Mix) was injected under the same analytical conditions in order to assign the chromatographic peaks and to estimate the amounts of acetone and aldehydes collected in the cartridges.

*Case of the closed photoreactor filled with $O_2$.* Direct analysis of the enclosed atmosphere was carried out with an Intersmat IGC 120FL gas chromatograph equipped with a flame ionization detector and a Vocol column (105 m long, 0.53 mm i.d., 3 μm film thickness) heated at 313 K. Identifications were confirmed by the use of the HP GC-MS apparatus equipped with a CP Wax 57 CB column (50 m long, 0.25 mm i.d., 1.2 μm film thickness) at 303 K, and operated in the electron ionization mode.

Solid phase micro-extraction (SPME) was used to adsorb the organic products contained in the enclosed atmosphere of

the photoreactor in order to detect analytes at lower concentrations. This technique[18,19] is an alternative to other concentration methods. It consists of two processes: partitioning of analytes between the silica fiber coating and the sample and desorption of concentrated analytes into an analytical instrument. Before each use, the fibers, purchased from Supelco, were thermally desorbed according to the supplier's instructions. The fiber holder assembly containing the retracted SPME fiber was introduced into the reactor through the septum. The fiber was exposed to the gaseous phase for various durations with the UV lamps on or off (see Results section). The fiber was then retracted into the holding assembly which was removed from the reactor and transferred to the injection port, set at 493 K, of the HP GC-MS apparatus equipped with a SPME inlet liner. The temperature of the same CP Sil 5 CB column was programmed from 313 K (hold time: 5 min) to 493 K at 5 K $min^{-1}$, and the electron ionization mode was used.

**2.4.4 $CO_2$ measurements.** Carbon dioxide was analyzed in the closed photoreactor by use of a catharometer gas-chromatograph (Intersmat, model IGC 20MB), equipped with a Porapak Q column (80–100 mesh, 3 m × 1/4 in).

In the case of the photoreactor through which a 50 mL $min^{-1}$ $O_2$ flow was circulated, the amount of $CO_2$ was too low to be measured in the exiting gas flow by gas chromatography. Consequently, we employed a chemical method: the gas flow was bubbled into three successive bottles containing each 200 mL of barium dihydroxide solution (1 mol $L^{-1}$). Carbon dioxide was precipitated as barium carbonate. The excess barium dihydroxide was titrated with potassium hydrogenphthalate (1.5 mol $L^{-1}$).

However, as volatile carboxylic acids produced by palmitic acid degradation also react with $Ba(OH)_2$, we thought it useful to also employ the following sequential procedure which allows one to measure, by gas chromatography, the $CO_2$ amounts produced. Palmitic acid-coated plates were placed into the photoreactor; the photoreactor was filled with dioxygen and closed; the plates were UV-irradiated during 1 h; $CO_2$ concentration in the photoreactor was then measured by GC; the photoreactor was filled again with dioxygen; the absence of $CO_2$ was checked. One-hour irradiation sequences were repeated until $CO_2$ was no longer emitted, *i.e.* the degradation of palmitic acid and its organic products were complete. The total amount of $CO_2$ corresponded to the amount of carbon dioxide produced in a periodically renewed atmosphere during the photocatalytic degradation of palmitic acid. Note that if a 50 mL $min^{-1}$ dioxygen flow was circulated through the reactor, the inner atmosphere was renewed about every 45 min. Therefore the sequential procedure we used can be considered as a satisfactory approximation to the situation in which dioxygen is permanently circulated.

## 3 Results

### 3.1 Photocatalytic disappearance of palmitic acid

When palmitic acid was deposited onto the non-$TiO_2$-coated side of the glass plates and UV irradiated under the conditions described above in the closed photoreactor, no decrease in the palmitic acid amount was observed after 15 h irradiation.

Disappearance of palmitic acid sprayed onto the $TiO_2$-coated side is shown in Fig. 5. Under our conditions, an apparent zero-order decay was observed with a rate constant $k = 0.60 \pm 0.12$ μmol $h^{-1}$, which means that an approximately 60 nm thick layer of palmitic acid was destroyed per hour. That removal was accompanied by a gradual improvement in the transparency of the glass plates according to visual estimations.

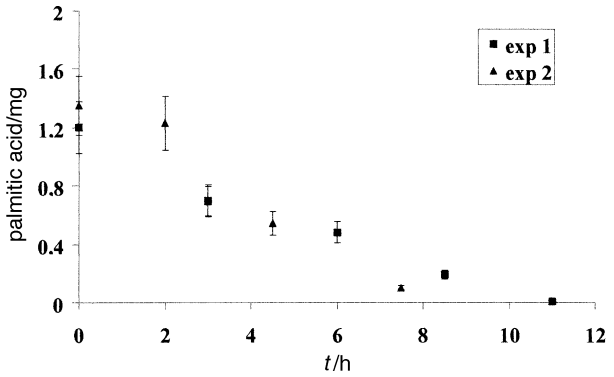


**Fig. 5** Photocatalytic disappearance of palmitic acid deposited on the self-cleaning glass plate; the two experiments give an idea of the reproducibility.

### 3.2 Identification of degradation intermediate products

Determining the nature and amount of the photooxidation products generated is required (i) to know whether this cleaning process may release into the atmosphere organic compounds which can be toxic or noxious, and (ii) to give an insight into the photocatalytic degradation pathways.

**3.2.1 Intermediate products detected on the glass plates.** A sodium hydroxide aqueous solution or dichloromethane were used to dissolve the products remaining on the glass plates. HPLC analysis of the NaOH solution indicated the presence of formic and acetic acids, whereas GC-MS analysis of the $CH_2Cl_2$ solution showed the presence of the five linear carboxylic acids containing 8 to 12 carbon atoms. The use of propan-1-ol instead of dichloromethane allowed the detection of tetradecanoic acid. Identifications were confirmed by use of standards.

**3.2.2 Intermediate products detected in the gas phase.** The various analytical techniques and procedures we employed allowed us to detect 39 products of palmitic acid degradation (Table 1) as is detailed below.

Under our laboratory conditions, experiments carried out in the closed photoreactor have had the advantage of allowing the identification of numerous intermediate products whose detection was impossible otherwise. In the real world, the atmosphere in the vicinity of a window glass plate is constantly changed whether we consider the outdoor or the indoor side, since renewing the atmosphere every hour is recommended in houses or buildings.[20] Consequently, we also thought it was necessary to determine the amount of volatile

**Table 1** Organic intermediate products (all linear) detected on the glass plates (P) or in the gas phase (G) during the photodegradation of palmitic acid deposited on self-cleaning glass plates

| | Alkanes | Primary alcohols | Aldehydes | Ketones | Acids |
|---|---|---|---|---|---|
| $C_1$ | | | G | / | P, G |
| $C_2$ | | | G | / | P, G |
| $C_3$ | | | G | G | G |
| $C_4$ | | | G | | G |
| $C_5$ | | | G | | G |
| $C_6$ | | | G | | G |
| $C_7$ | G | G | G | | G |
| $C_8$ | G | G | G | | G |
| $C_9$ | G | | G | | P, G |
| $C_{10}$ | G | | G | | P, G |
| $C_{11}$ | G | | G | | P, G |
| $C_{12}$ | G | | G | | P, G |
| $C_{13}$ | G | | G | | G |
| $C_{14}$ | G | | G | | P |
| $C_{15}$ | G | | | | |

organic compounds released during palmitic acid degradation under the conditions where $O_2$ flow through the photoreactor was at a velocity corresponding to this renewal rate.

Acetone, pentanal, hexanal, heptane and octane produced during the photodegradation of palmitic acid sprayed on the glass plates were trapped into cartridges containing activated carbon and identified by GC-MS analysis.

Adsorption/reaction of carbonyl products in cartridges containing 2,4-DNPH-coated $SiO_2$ allowed the detection of acetone and $C_1$–$C_6$ linear aldehydes. Only trace amounts were adsorbed in the second cartridge (see Experimental section), which showed that the levels of carbonyl products in the first cartridge did not reach the saturation limit and therefore that the expected carbonyl products were quantitatively collected in the first cartridge. The estimated amounts formed from $0.57 \pm 0.08$ μmol palmitic acid are indicated in Table 2. Formaldehyde and acetaldehyde were formed in higher amounts than the other linear aldehydes, in particular $C_4$–$C_6$ linear aldehydes were found in trace amounts. The sum of the amounts of acetone and $C_1$–$C_3$ linear aldehydes emitted under these conditions represented $22 \pm 4\%$ of the amount of organic carbon initially present in the photoreactor. Note that acrolein (propenal) and crotonaldehyde (buten-2-al) would have been detected if they had been produced in amounts $>0.5$ μg from 0.15 mg palmitic acid.

The amounts of acetone and acetaldehyde were sufficient to monitor their concentration by GC-FID (Fig. 6) in the enclosed atmosphere of the photoreactor (note that formaldehyde cannot be detected by FID). The maximum detected amounts of acetone (*ca.* 4.5 μmol) and acetaldehyde (*ca.* 7 μmol) were obtained when *ca.* 70% of palmitic acid was eliminated (Fig. 6). The photoreactor initially contained about $5 \times 1.5$ mg of palmitic acid, *i.e. ca.* 30 μmol. The lower ratio of the amount of acetaldehyde to that of actone in the closed photoreactor than when oxygen was circulated (Table 2) is consistent with the better stability of acetone toward oxidation.

Analysis of the enclosed atmosphere carried out with SPME-GC-MS led to the detection and the identification of numerous volatile intermediate products. Every linear carboxylic acid containing from 1 to 12 carbon atoms was detected by use of a 85 μm polyacrylate fiber. A 65 μm polydimethylsiloxane–divinylbenzene (PDMS–DVB) fiber enabled the detection of 29 products (Fig. 7): four linear alkanes (from $C_{12}$–$C_{15}$), two linear primary alcohols ($C_7$ and $C_8$), acetone, ten linear aldehydes (from $C_5$ to $C_{14}$) and twelve linear carboxylic acids ($C_1$, $C_2$ and $C_4$ to $C_{13}$).

A control experiment was carried out with palmitic acid deposited onto the non-$TiO_2$-coated side. Analysis of the enclosed atmosphere with the PDMS–DVB fiber showed that some unidentified peaks in the chromatogram obtained under the usual operating conditions were in fact due to compounds released from the fiber under UV irradiation; but the aforementioned products were not found in this control experiment.

To ensure that all the identified products were not generated by interactions between the fiber phase and some analytes when irradiating during 15 h, another experiment was carried out. Instead of leaving the fiber in the photoreactor during the whole photodegradation, the fiber was exposed to the enclosed atmosphere of the photoreactor during only 15 min, in the dark, after having irradiated the glass plates for various durations. Under these conditions, the previously identified products were also detected, which confirmed they were intermediate products of palmitic acid degradation. However, the chromatographic peaks were less numerous and less intense (compare Fig. 8 and 7). On one hand, $C_8$–$C_{13}$ acids and $C_9$–$C_{14}$ aldehydes were not detected possibly because it took a longer time for these less volatile compounds to equilibrate with the fiber coating. On the other hand butanal, nonane, decane and undecane were detected; these products are, within their chemical category, more volatile than those observed when the fiber was continuously exposed to the photoreactor atmosphere.

These short exposure-time SPME-analyses brought some information on the chronological order of formation of the intermediate products. For example, butanoic acid was detected in the chromatogram obtained after 1 h irradiation, whereas propanoic acid and acetic acid were detected in the chromatograms obtained after 2.5 and 5.5 h irradiation, respectively. Among the carboxylic acids, the shorter ones were not surprisingly emitted later than the longer ones, which revealed the gradual splitting of the palmitic acid chain (*e.g.* compare the chromatograms shown in Fig. 8).

**Table 2** Estimated amounts of acetone and $C_1$–$C_3$ linear aldehydes released from $0.57 \pm 0.08$ μmol of palmitic acid under a 50 mL $min^{-1}$ $O_2$ flow

| Product | Released amount/μmol |
|---|---|
| Acetone | $0.13 \pm 0.01$ |
| Formaldehyde | $0.34 \pm 0.05$ |
| Acetaldehyde | $0.59 \pm 0.09$ |
| Propanal | $\approx 0.05$ |

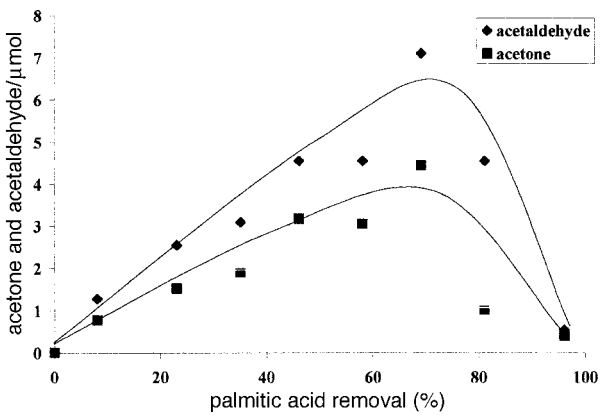


**Fig. 6** Temporal variations in the amounts of acetone and acetaldehyde in the closed photoreactor during palmitic acid (initial amount: 30 μmol) degradation.

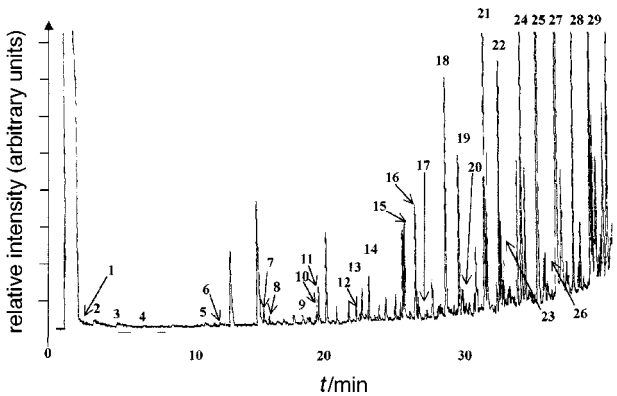


**Fig. 7** GC chromatogram, obtained after 15 h adsorption on a polydimethylsiloxane–divinylbenzene 65 μm fiber, of the products emitted into the gas phase during palmitic acid degradation. Identification performed by mass spectrometry. Irradiation duration: 15 h. 1, acetone; 2, formic acid; 3, acetic acid; 4, pentanal; 5, hexanal; 6, butanoic acid; 7, heptanal; 8, pentanoic acid; 9, heptan-1-ol; 10, hexanoic acid; 11, octanal; 12, octan-1-ol; 13, heptanoic acid; 14, nonanal; 15, octanoic acid; 16, decanal; 17, dodecane; 18, nonanoic acid; 19, undecanal; 20, tridecane; 21, decanoic acid; 22, dodecanal; 23, tetradecane; 24, undecanoic acid; 25, tridecanal; 26, pentadecane; 27, dodecanoic acid; 28, tetradecanal; 29, tridecanoic acid.

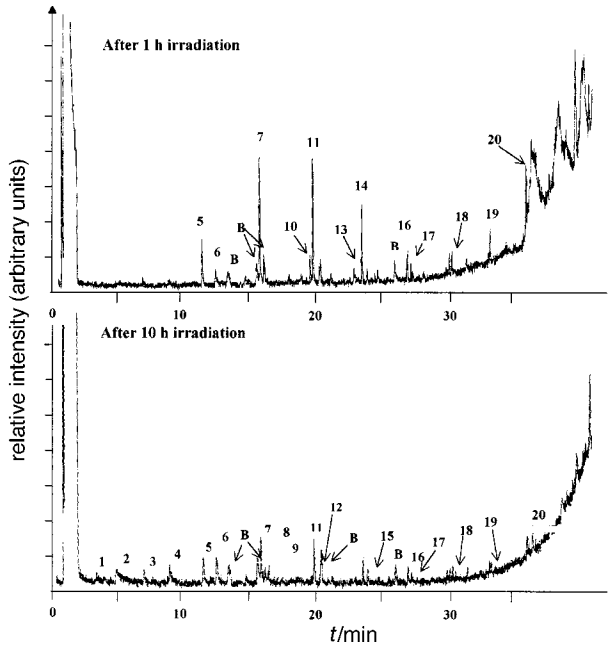


**Fig. 8** GC chromatogram, obtained after 15 min adsorption on a PDMS–DVB 65 μm fiber, of the products emitted into the gas phase during palmitic acid degradation. Product identification by mass spectrometry. 1, butanal; 2, acetic acid; 3, pentanal; 4, propanoic acid; 5, hexanal; 6, butanoic acid; 7, heptanal; 8, pentanoic acid; 9, nonane; 10, hexanoic acid; 11, octanal; 12, decane; 13, heptanoic acid; 14, nonanal; 15, undecane; 16, decanal; 17, dodecane; 18, tridecane; 19, tetradecane; 20, pentadecane; B, this peak was present in the blank analysis.

None of the intermediate products were found in two types of control experiments, *i.e.* without UV irradiation or when palmitic acid was deposited on the non-$TiO_2$-coated side of the plates.

### 3.3 Mass balance

Quantification in the enclosed atmosphere showed that, after a regular increase within at least the first 10 h of irradiation, $CO_2$ concentration reached a plateau after *ca.* 22 h (Fig. 9). The amount of palmitic acid initially introduced was $29 \pm 4$ μmol, which potentially corresponded to $0.47 \pm 0.07$ mmol $CO_2$, whereas $0.38 \pm 0.04$ mmol $CO_2$ were found to be emitted according to our measurements. Considering these accuracies, the mineralization of palmitic acid can be regarded as being complete when the photocatalytic degradation took place in the closed photoreactor.

When $CO_2$ was quantified in the 50 mL $min^{-1}$ $O_2$ flow coming out from the reactor after trapping in barium dihydroxide solutions, the conversion rate from palmitic acid into $CO_2$ was estimated to be $80 \pm 15\%$.

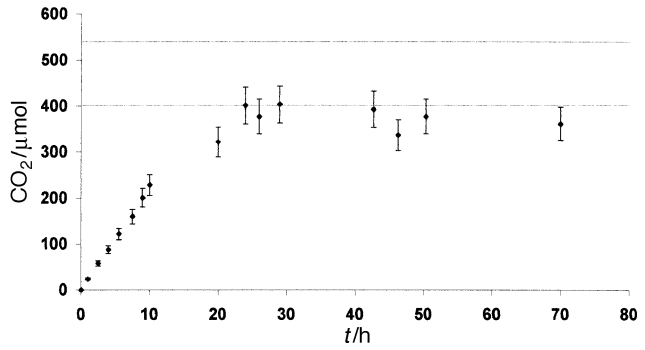


**Fig. 9** Production of $CO_2$ during the photocatalytic degradation of palmitic acid in the closed photoreactor. Horizontal lines: maximum and minimum (considering the accuracy in the amount of deposited palmitic acid) of $CO_2$ expected from complete mineralization.

When $CO_2$ was quantified in the periodically renewed atmosphere, because of an increase in the total uncertainty (*ca.* 25%) resulting from the addition of $CO_2$ amounts measured separately, the conversion of palmitic acid into $CO_2$ was evaluated to be comprised between 72 and 100%. Note that, under these conditions, volatile organic products were eliminated when the atmosphere was renewed and thereby could not be mineralized.

The two results obtained for the conversion of palmitic acid into $CO_2$ are consistent. We can conclude that the conversion into $CO_2$ lies between 72 and 95% if we consider the overlap between the ranges evaluated by the two types of measurements.

We also tried to evaluate the total amount of the products that were detected with the PDMS–DVB SPME fiber. For that purpose, a solution in dichloromethane of linear $C_9$–$C_{15}$ alkanes, $C_7$–$C_{14}$ aldehydes (which were the aldehydes not quantified by use of the 2,4-DNPH-coated silica cartridges, *cf.* Table 2) and $C_4$–$C_{13}$ acids was analyzed under the same conditions as those used to analyze the products collected on the fiber. From this analysis we deduced that the amounts, collected on the fiber, of all these products corresponded to only *ca.* 0.01% of the organic carbon initially present in the photoreactor. Even if we assume that only a small percentage of these volatile organics (say 1%, to be very pessimistic) were collected on the fiber, we can infer that less than 1% of the palmitic acid carbon was emitted as linear $C_9$–$C_{15}$ alkanes, $C_7$–$C_{14}$ aldehydes and $C_4$–$C_{13}$ acids.

In short, under the conditions corresponding to the renewal of the photoreactor atmosphere every hour, the mass balance from palmitic acid photocatalytic degradation on the $TiO_2$-coated glass plates is the following (expressed in percentages of the palmitic acid carbon):

(*a*) $CO_2$: 72–95%;
(*b*) acetone, acetaldehyde and formaldehyde: $22 \pm 4\%$;
(*c*) linear alkanes ($C_9$–$C_{15}$), aldehydes ($C_7$–$C_{14}$) and acids ($C_4$–$C_{13}$): maximum 1%.

Amounts of volatile carboxylic acids and alkanes were not estimated. However, the sum of the amounts of $CO_2$, acetone and $C_1$–$C_6$ linear aldehydes represented between 91 and 100% of the carbon amount initially contained in palmitic acid. This means the amounts of products which were not detected or quantified corresponded to $<9\%$ of the carbon contained in palmitic acid.

## 4 Discussion

### 4.1 Palmitic acid elimination. Glass self-cleaning efficiency

The zero-order degradation kinetics for palmitic acid disappearance was consistent with the constant saturation of the $TiO_2$ surface by the palmitic acid molecules which were sprayed on the top layer of $TiO_2$ nanoparticles (Fig. 1).

We have shown that, despite the fact that the self-cleaning glass was not optimized and despite the chemical stability of palmitic acid, layers of several tens of nm of this compound could be destroyed under solar-like irradiation. This corresponded to a quantum yield of the order of 0.002 (with respect to UV-A photons incident on the plates) as usual in photocatalysis. Palmitic acid removal was accompanied by a gradual improvement in the transparency of the glass plates according to visual estimations (Fig. 10). This result illustrates the efficiency of the $TiO_2$-coated glass to clean itself from a compound representative of grease stains.

This efficiency was further demonstrated by the mass balance. In the closed photoreactor, palmitic acid could be totally mineralized within experimental accuracy. When an oxygen flow was circulated through the photoreactor to simulate more realistic conditions, palmitic acid and its interme-

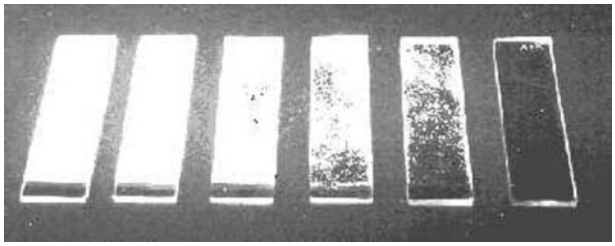

**Fig. 10** Visual aspect of glass plates initially covered with *ca.* 6 mg palmitic acid, after increasing irradiation durations (from left to right: 0, 8, 16, 24, 32, 40 h UV irradiation in the photoreactor).

diate products of higher molecular weight were transformed principally into $CO_2$ and also into a few VOCs (Table 2) swept out from the reactor and corresponding to about 22% of palmitic acid carbon under our conditions.

### 4.2 Influence on indoor air quality

Because of the huge dilution capacity of the troposphere, VOCs formed from palmitic acid and related compounds contained in grease stains on glass panes, will obviously not affect the outdoor air quality. However, the question may be relevant for indoor air.

Assuming that the amounts of acetone, formaldehyde and acetaldehyde listed in Table 2 are suddenly released in a 24 $m^3$-room at *ca.* 293 K , the concentrations in ppbv of these products would be 0.13 (acetone), 0.34 (formaldehyde) and 0.59 (acetaldehyde). These values are 35–125 times lower than the average concentrations in ppbv reported for indoor air in buildings: for instance 8.6 (acetone),[21] 42 (formaldehyde)[21] and 21 (acetaldehyde).[22] In other words, the perturbation in air quality would become significant only for a quantity of palmitic acid about 35 times greater than that corresponding to Table 2 (*ca.* 0.57 μmol). This latter quantity represented a palmitic acid mean thickness of *ca.* 60 nm on a 30 $cm^2$-plate and gave the visual impression of a quite dirty glass. That means that the air quality might be significantly altered if a 60 nm-thick layer of palmitic acid covered in the order of $35 \times 30$ $cm^2 = 0.105$ $m^2$ of glass pane, *i.e. ca.* 7% of the window panes (*ca.* 1.5 $m^2$) in a 24 $m^3$-room.

Unfortunately, to our knowledge, data about the amounts of organic material present on indoor glass surfaces are lacking. Accordingly, we cannot indicate whether the dirt level we calculated might be reached. In general, window panes gradually become dirty, and moreover the cleaning process of the $TiO_2$-coated glasses being continuous, the resulting oxidized VOCs will be released progressively and not suddenly, as assumed in our calculations, so that these calculations correspond to upper limit concentrations.

In addition, the clean part of the $TiO_2$-coated glass panes can adsorb the VOCs and mineralize them as illustrated by our experiments in the closed photoreactor. However, on the other hand, adsorption on the $TiO_2$-coated glass of hydrocarbons contained in indoor air and subsequent photocatalytic transformations of these substances will both decrease the hydrocarbon concentrations and contribute to increase the concentrations in oxygenated VOCs produced from the hydrocarbons if the formation rate of these oxidized products dominated their mineralization rate. This is another debate.

The only purpose for the comparison between the amounts of carbonyl products formed from palmitic acid and the concentrations in these products usually present in indoor air was to provide some data illustrating under what conditions an unfavorable influence of the self-cleaning glasses upon air quality might appear. However, in the absence of knowledge about dirt levels formed on glass panes from both continuous and irregular sources, it is impossible to tell whether these conditions might be met.

### 4.3 Remarks on the detection of intermediate products

As is detailed in the Results section, numerous intermediate products of the photodegradation of palmitic acid on the $TiO_2$-coated glass plates have been identified (Table 1). However, it would be naive to claim that the list of these products is complete. Indeed, detection of analytes is strongly dependant on the analytical technique. For instance, the whole range of $C_1$–$C_{14}$ linear carboxylic acids were detected in the atmosphere of the photoreactor. Some of these carboxylic acids were detected on the glass plates as well: formic and acetic acids dissolved in a NaOH solution, $C_8$–$C_{12}$ acids dissolved in $CH_2Cl_2$, and tetradecanoic acid dissolved in propan-1-ol. It is obvious that the carboxylic acids containing from three to seven carbon atoms were also present on the glass plates as a result of an equilibrium between the adsorbed/deposited phase and the gas phase for each product. However, only the products that were present in a sufficient amount on the plates and that were soluble enough in the solvents we used were detected on the plates. Also, when a plate was taken out of the photoreactor, the equilibrium between the adsorbed and the gaseous phase was modified and only strongly adsorbed and/or weakly volatile products remained on the plates.

Therefore we consider that palmitic acid yielded the whole series of linear $C_{15}$–$C_1$ aldehydes, acids and alkanes (no attempt was made to detect $C_6$–$C_1$ alkanes because they were quantitatively negligible given the mass balance). We also think that primary alcohols were formed in very low amounts, so that only heptan-1-ol and octan-1-ol could be detected.

### 4.4 Suggested degradation pathways

Analyzing the intermediate products at different stages of the degradation showed the gradual splitting of palmitic acid. Degradation pathways are considered hereafter to explain the formation of these intermediate products.

Reaction of carboxylic acids with a photogenerated hole leads to decarboxylation.[23–25] This reaction could be favored by the interaction of these acids with the $TiO_2$ surface *via* the carboxyl group [eqn. (1), R = $CH_3(CH_2)_{14}$ for palmitic acid].

$$RCH_2CO_2H + h^+ \rightarrow RCH_2^{\cdot} + CO_2 + H^+ \quad (1)$$

Easy addition of dioxygen to the alkyl radical would yield the corresponding alkylperoxyl radical [eqn. (2)]

$$RCH_2^{\cdot} + O_2 \rightarrow RCH_2OO^{\cdot} \quad (2)$$

According to literature, $RCH_2OO^{\cdot}$ can (i) abstract an H atom from a molecule[26] *e.g.* palmitic acid (or possibly from another molecule depending on the stage the cleaning process has reached) to produce a hydroperoxide $RCH_2OOH$, and (ii) combine either with an identical or non-identical alkylperoxyl radical[27–30] or with a hydroperoxy radical formed either from conduction band electrons, dioxygen and protons [eqn. (3) or *via* eqn. (7) (below)]

$$e^- + O_2 \rightarrow O_2^{\cdot -} \qquad O_2^{\cdot -} + H^+ \rightleftharpoons HO_2^{\cdot} \quad (3)$$

Tetroxides $(RCH_2)_2O_4$, $RCH_2$–$O_4$–$CH_2R'$ or $RCH_2O_4H$ are believed to be generated in that latter case.[31,32] However, in the condensed phase the production of hydroperoxides should predominate over radical recombination as a result of the high pool of nontransformed molecules, provided they contain labile H atoms.

Hydroperoxides are photochemically stable in the spectral range used, so they can decompose only thermally [eqn. (4) and (5)].[26,29]

$$RCH_2OOH \rightarrow RCH_2O^{\cdot} + OH^{\cdot} \quad (4)$$

$$2RCH_2OOH \rightarrow RCH_2O^{\cdot} + RCH_2OO^{\cdot} + H_2O \quad (5)$$

The resulting alkoxy radical could undergo several reactions [eqn. (6)–(9)].[26,29,30]

$$RCH_2O^{\cdot} + R'H \rightarrow RCH_2OH + R'^{\cdot} \quad (6)$$

$$RCH_2O^{\cdot} + O_2 \rightarrow RCHO + HO_2^{\cdot} \quad (7)$$

$$RCH_2O^{\cdot} \rightarrow HCHO + R^{\cdot} \quad (8)$$

$$2RCH_2O^{\cdot} \rightarrow RCH_2O\text{–}OCH_2R \quad (9)$$

The peroxides supposed to be produced *via* the latter reaction could not be detected under our analytical conditions.

The same types of products could be formed from the tetroxide $(RCH_2)_2O_4$, either directly [eqn. (10)–(12)][32] or through the radical $RCH_2O^{\cdot}$ generated by reaction (13).

$$(RCH_2)_2O_4 \rightarrow RCHO + RCH_2OH + O_2 \quad (10)$$

$$(RCH_2)_2O_4 \rightarrow 2RCHO + H_2O_2 \quad (11)$$

$$(RCH_2)_2O_4 \rightarrow 2HCHO + 2R^{\cdot} + O_2 \quad (12)$$

$$(RCH_2)_2O_4 \rightarrow 2RCH_2O^{\cdot} + O_2 \quad (13)$$

In the case of the tetroxide $RCH_2O_4H$, reactions equivalent to reactions (10) and (13) could occur [eqn. (14) and (15)].

$$RCH_2O_4H \rightarrow RCHO + H_2O + O_2 \quad (14)$$

$$RCH_2O_4H \rightarrow RCH_2O^{\cdot} + OH^{\cdot} + O_2 \quad (15)$$

Eqn. (4)–(15) show that aldehydes, in particular formaldehyde, and primary alcohols can be formed from the alkylperoxy radicals obtained through reaction (2). These pathways assume the formation of either hydroperoxides and/or tetroxides and the subsequent thermal decomposition of these species. Aldehydes can easily be oxidized to the corresponding acids. Alkyl radicals [eqn. (6), (8) and (12)] can recombine to yield alkanes. Therefore these pathways allows one to account for all the products of palmitic acid degradation we detected except acetone.

Concerning the formation of hydroperoxides, palmitic acid, at least initially, should be the main source of H atoms in the reaction [eqn. (16)].

$$RCH_2O_2^{\cdot} + R'H \rightarrow RCH_2OOH + R'^{\cdot} \quad (16)$$

Considering the bond strengths, H abstraction should involve one of the $CH_2$ groups in palmitic acid, and the resulting alkyl radicals would lead to carbonylated acids, and subsequently diacids, through pathways equivalent to those presented above. Carbonylated acids and diacids were not detected at least under our analytical conditions. We therefore hypothesize that the carboxylic H atom could be predominantly abstracted possibly because of its proximity to the $TiO_2$ surface and because of a weakening of the COO–H bond strength due to adsorption. The resulting radical would readily decarboxylate [eqn. (17)]

$$R'^{\cdot} = RCH_2COO^{\cdot} \rightarrow RCH_2^{\cdot} + CO_2 \quad (17)$$

giving an alkyl radical equivalent to that obtained by reaction of a photogenerated hole with palmitic acid or with the acids subsequently produced [eqn. (1)].

The same hypothesis can be evoked regarding the role of hydroxyl radicals. These radicals can be formed during the photocatalytic process when a photogenerated hole is trapped by a water molecule.

$$h^+ + H_2O \rightarrow OH^{\cdot} + H^+ \quad (18)$$

They could also be produced from hydroperoxides [eqn. (4)] and $RCH_2O_4H$ tetroxides [eqn. (15)]. If they abstracted H atoms from the $CH_2$ groups in palmitic acid, carbonylated acids and diacids would be expected. Because these products were not observed, we again suggest that H abstraction mainly occurred at the $CO_2H$ group as in the case where the H abstracting radical is $RCH_2OO^{\cdot}$ [eqn. (19)]

$$RCH_2CO_2H + OH^{\cdot} \rightarrow RCH_2COO^{\cdot} + H_2O \quad (19)$$

which would subsequently give rise to radical $RCH_2^{\cdot}$ [eqn.(17)]. Consequently, product analysis does not allow one to discriminate between an initial attack of palmitic acid by a hole [eqn. (1)] or a hydroxyl radical [eqn. (19)]. In addition, $OH^{\cdot}$ and $RCH_2OO^{\cdot}$ radicals can abstract H atoms from the aldehydic groups and less easily from the $CH_2$ groups in alkanes.

Formation of acetone (Figs. 6 and 7, Tables 1 and 2) is not directly accounted for by the reactions suggested above for the fate of alkylperoxy radicals. If acetone was formed only *via* the combination of an acetyl radical, derived from acetaldehyde, and a methyl radical, other ketones would be reasonably expected to be produced from equivalent radicals with a higher number of C atoms; no ketone but acetone was found though our analytical methods were appropriate for detecting higher ketones. This difficulty in explaining the formation of acetone indicates that the mechanisms suggested are not comprehensive even if they account for the formation of all the other products.

## 5 Conclusion

Our results show that layers of some tens of nm of fatty acids (*i.e.* a few tens of nmol $cm^{-2}$), such as palmitic acid, can be removed within hours under solar-like irradiation of the anatase-coated glass plates we used. As analyses carried out in our laboratory have indicated that a thumb print on glass contains between 0.5 and 1.5 nmol $cm^{-2}$ of palmitic acid, self-cleaning from this type of stain will indeed be very rapid even on a cloudy day. Furthermore, progress is expected in the efficiency of the $TiO_2$-coating which was not optimized.

Two main conclusions can be drawn from our analyses of the products of palmitic acid. From the practical viewpoint, our study showed that more than 72% of palmitic acid was converted into $CO_2$, when the photoreactor atmosphere was renewed every hour. The majority of the organic products identified were present at negligible concentrations in the gas phase. Only formaldehyde, acetaldehyde and acetone were found at higher levels; *ca.* 22% of palmitic acid carbon was converted into these three products. From the fundamental viewpoint, the absence of ramified compounds and of carbonylated or hydroxylated acids among the products has led us to suggest that the reacting site of palmitic acid (and other acids formed from it) is the carboxylic group.

To complete these data, an on-going study addresses the case of a still more stable compound which represents organic deposits emanating from other sources.

## Acknowledgements

V. R. is grateful to the CNRS and to Rhône-Poulenc for her Ph.D. scholarship. We thank Rhône-Poulenc for partial financial support and Saint-Gobain for preparing the $TiO_2$-coated glass plates.

## References

1 See for example: P. Pichat, in *Handbook of Heterogeneous Catalysis*, ed. G. Ertl, H. Knözinger and J. Weitkamp, Wiley-VCH, Weinheim, 1997, vol. 4, pp. 2111–2122.
2 H. Cui, H. S. Shen, Y. M. Gao, K. Dwight and A. Wold, *Mater. Res. Bull.*, 1993, **28**, 195.
3 Y. Paz, Z. Luo, L. Rabenberg and A. Heller, *J. Mater. Res.*, 1995, **10**, 2842.
4 N. Neigishi, T. Iyoda, K. Hashimoto and A. Fujishima, *Chem. Lett.*, 1995, 841.
5 A. Fujishima, K. Hashimoto, T. Iyoda and S. Fukayama, *Eur. Pat. Appl.*, 0 737 513 A1, 1996.
6 Saint-Gobain Vitrage, *Fr. Pat.* 95 10839, published in BOPI no. 12, March 1997.

7 Super-hydrophilic photocatalyst and its applications, TOTO Ltd; Photocatalyst project team, Toto web site: http://www.toto.co.jp/Hydro-E/hydro1-E.htm
8 A. Fujishima, *Look Jpn*., 1995, **41**, 471.
9 A. Heller, *Acc. Chem. Res*., 1995, **28**, 503.
10 P. Boulanger, F. Tayeau, P. Mandel and G. Biserte, *Biochimie Médicale I*, Masson, Paris, 1962, p. 534.
11 S. B. Hawthorne, D. J. Miller, J. Pawliszyn and C. L. Arthur, *J. Chromatogr*., 1992, **603**, 185.
12 W. F. Rogge, L. M. Hildemann, M. A. Mazurek, G. R. Cass and B. R. T. Simoneit, *Environ. Sci. Technol*., 1991, **25**, 1112.
13 M. R. Guerin, R. A. Jenkins and B. A. Tomkins, *The Chemistry of Environmental Tobacco Smoke, Composition and Measurements*, L. Clar, Chelsea, MI, 1992, pp. 43–61.
14 W. F. Rogge, M. A. Mazurek, L. M. Hildemann, G. R. Cass and B. R. T. Simoneit, *Atmos. Environ*., 1993, **27**, 1309.
15 S. Sitkiewitz and A. Heller, *New J. Chem*., 1996, **20**, 233.
16 L. R. Koller, *Ultraviolet Radiation*, Wiley & Sons, New York, 1965, ch. 4.
17 J.-M. Herrmann, J. Disdier, P. Pichat, S. Malato and J. Blanco, *Appl. Catal. B*, 1998, **17**, 15.
18 Z. Zhang, M. J. Yang and J. Pawliszyn, *Anal. Chem*., 1994, **66**, 844.
19 J. Pawliszyn, *Solid Phase Microextraction, Theory and Practice*, Wiley-VCH, New York, 1997.
20 L. Molhave, B. Bach and O. F. Pedersen, *Environ. Int*., 1986, **12**, 167.
21 J. J. Shah and H. B. Singh, *Environ. Sci. Technol*., 1988, **22**, 1381.
22 A. H. Miguel, F. R. de Aquino Neto, J. N. Cardoso, P. de C. Vasconcellos, A. S. Pereira and K. S. G. Marquez, *Environ. Sci. Technol*., 1995, **29**, 338.
23 B. Kraeutler and A. J. Bard, *J. Am. Chem. Soc*., 1977, **99**, 7729.
24 H. L. Chum, M. Ratcliff, F. L. Posey, J. A. Turner and A. J. Nozik, *J. Phys. Chem*., 1983, **87**, 3089.
25 Y. Mao, C. Schöneich and K. D. Asmus, *J. Phys. Chem*., 1991, **95**, 10080.
26 R. A. Larson and E. J. Weber, *Reactions Mechanisms in Environmental Organic Chemistry*, Lewis, Boca Raton, FL, 1994, ch. 4.
27 A. F. Marchaj, D. G. Kelley, A. Bakac and J. H. Espenson, *J. Phys. Chem*., 1991, **95**, 4441.
28 A. F. Wagner, I. R. Slagle, D. Sarzynski and D. Gutman, *J. Phys. Chem*., 1990, **94**, 1853.
29 P. D. Lightfoot, R. A. Cox, J. N. Crowley, M. Destriau, G. D. Hayman, M. E. Jenkin, G. K. Moortgat and F. Zabel, *Organic Peroxy Radicals*, Commission of the European Communities, Brussels, 1993.
30 R. Atkinson, *Int. J. Chem. Kinet*., 1997, **29**, 99.
31 J. E. Bennett and J. A. Howard, *J. Am. Chem. Soc*., 1973, **95**, 4008.
32 C. von Sonntag and H.-P. Schuchmann, *Angew. Chem., Int. Ed. Engl*., 1991, **30**, 1229.

*Paper 9/01342C*